# Flexibility Potential of Space Heating Demand Response in Buildings for District Heating Systems

(article starts on next page)

# Flexibility Potential of Space Heating Demand Response in Buildings for District Heating Systems

**Dmytro Romanchenko *** , **Emil Nyholm, Mikael Odenberger and Filip Johnsson**

Department of Space, Earth and Environment, Chalmers University of Technology, S412 96 Göteborg, Sweden
* Correspondence: dmytror@chalmers.se; Tel.: +46-(0)31-772-1432

**Abstract:** Using an integrated demand-supply optimization model, this work investigates the potential for flexible space heating demand, i.e., demand response (DR), in buildings, as well as its effects on the heating demand and the operation of a district heating (DH) system. The work applies a building stock description, including both residential and non-residential buildings, and employs a representation of the current DH system of the city of Gothenburg, Sweden as a case study. The results indicate that space heating DR in buildings can have a significant impact on the cost-optimal heat supply of the city by smoothing variations in the system heat demand. DR implemented via indoor temperature deviations of as little as +1 °C can smoothen the short-term (daily) fluctuations in the system heating demand by up to 18% over a period of 1 year. The smoothening of the demand reduces the cost of heat generation, in that the heat supply and number of full-load hours of base-load heat generation units increase, while the number of starts for the peaking units decreases by more than 80%. DR through temperature deviations of +3 °C confers diminishing returns in terms of its effects on the heat demand, as compared to the DR via +1 °C.

**Keywords:** district heating; energy demand; buildings; demand response; optimization; modeling

## 1. Introduction

Energy use in buildings accounts for about one-third of the total global energy use. The International Energy Agency (IEA) estimates that if no action is taken to improve energy efficiency in this sector energy consumption in buildings will rise by almost 50% between 2010 and 2050 due to the expansion of the sector [1]. Thus, improving the energy efficiency and decreasing the energy demand of buildings are crucial factors in reaching global sustainability targets. Furthermore, buildings that are equipped with advanced control systems permit the smart control of energy loads, thereby conferring flexibility on the supply side via an active demand response (DR), e.g., the shifting of the electricity consumption of electrical appliances, including heating [2] or smart charging of electric vehicles [3]. The largest share of energy use in EU households, 79%, is for space heating and hot-water use [4]. In Sweden, about 55% of the heating demand of all buildings and up to 92% of the demand in multi-family residential houses are supplied by district heating (DH) [5]. DH systems in Sweden experience significant variations in heating demand (including long-term seasonal and short-term daily variations). This results in part-load operations of base- and mid-load heat generation units and frequent starting and stopping of peaking units, which are often fossil-fueled, heat-only boilers (HOB). In Year 2013, around 40% of the total heat generation in Swedish DH systems was from Combined Heat and Power (CHP) plants and around 8% was from Heat Pumps (HPs) [6] using waste heat as the heating source. The utilization of CHP plants and HPs in DH systems represents a strong linkage between the heat and electric power systems. Thus, DR from buildings has the potential to provide flexibility services, both directly to DH systems and indirectly to the power system via the smart

operation of CHP plants and HPs. The expected increase in non-dispatchable electricity generation, in the form of wind and solar power, means that the demand for flexibility will increase.

Hot-water use in buildings usually reflects social factors, i.e., the preferences of the inhabitants, and is therefore presumed to have limited potential in terms of providing flexibility services. In contrast, active DR from space heating, achieved through the utilization of thermal energy storage, is contrary and is considered to be an available and effective flexibility measure [7,8].

Modeling studies that investigate the flexibility potential of DR in buildings adopt two main approaches: (1) DR is achieved as a response to a fixed external signal, e.g., an electricity price vector over time, and thus, no feedback loops from the demand to the supply side are accounted for; and (2) the effect of flexible demand is accounted for by interchanging (i.e., soft- or hard-linking) the calculations of demand and generation, e.g., using integrated demand-supply models.

The studies of Finck et al. [9], Stinner et al. [8], and Hewitt [10] all employed the first of these modeling approaches to study the potential of demand-side flexibility for the electric power system in the forms of power-to-heat conversion via HPs and Thermal Energy Storage (TES) in hot-water tanks. In addition (or as an alternative) to hot-water tanks, TES can exploit the thermal mass of buildings to store heat by allowing for indoor temperature deviations from the set-point temperature, provided that the comfort requirements of the inhabitants are retained [11,12]. Reynders et al. [13] have proposed a simulation-based quantification method for the characterization of the DR potential via structural TES in buildings, and have used that approach to demonstrate the relationship between building properties (e.g., U-value) and its flexibility potential for the electric power system [13,14]. The studies of Dreau and Heiselberg [15], Halvgaard et al. [16], Pedersen et al. [17], and Masy et al. [18] evaluated thermal behavior and the potential for energy shifting in buildings with electric heating under different control strategies, although they did not include feedback loops from the demand side. All these studies reported economic benefits from applying DR in the heating system, while Pedersen et al. [17] also reported reductions in $CO_2$ emissions associated with reduced heating in buildings as a result of DR. Ingvarsson and Werner [19] and Kensby et al. [20] evaluated the changes in indoor temperature and space heating demand arising from adjustments in the control signal from the outdoor temperature sensor in multi-family buildings connected to DH. Ingvarsson and Werner [19] concluded that multi-family buildings utilized as TES could eliminate daily heat load variations in DH systems. Kensby et al. [20] showed that such utilization of the multi-family building stock (BS) could be achieved while complying with the indoor temperature comfort requirements, i.e., the thermal capacity of the buildings was estimated to be 0.1 kWh/m²$_{heated\ area}$ when limiting indoor temperature deviations to ±0.5 °C.

In the second modeling approach, Patteeuw et al. [21] developed a model that integrates (by soft-linking) a physical demand-side model, which includes an HP and an electric heater and building TES, with a traditional supply-side unit commitment model of the electric power system. In this model, the electric power system was represented by 26 electricity-generating units, including nuclear, coal-fired, and gas-fired power plants, and the demand from the building stock was represented by scaling up 25 identical buildings with different user behaviors and numbers of inhabitants. They concluded that it is important to include the feedback mechanism between the supply and demand sides to describe the effects of elastic demand, in the form of DR, on the supply side. The potential DR from buildings with electric space heating (both HP and direct electric heating) has been investigated by Papaefthymiou et al. [22], Hedegaard and Balyk [23], and Nyholm et al. [24]. All three studies applied detailed thermal building models that were integrated with economic dispatch models of the electricity systems in Germany, Denmark, and Sweden, respectively. These studies have shown that active DR from investigated building stocks has the potential to benefit the power system by: i) Presenting a viable and competitive alternative to other electricity storing technologies, e.g., pumped hydro (Papaefthymiou et al. [22]); ii) reducing the need for peak and reserve capacity investments (Hedegaard and Balyk [23]); and iii) decreasing the numbers of starts and stops and the degrees of

part-load operation of thermal power plants, and decreasing the operation time of peaking power plants (Nyholm et al. [24]), all of which lead to a decreased system cost.

　　When it comes to DH systems and the interactions between DR in buildings, heat generation in DH systems, and electricity generation in electric power systems has been studied by Pan et al. [25], Gu et al. [26], and Li et al. et al. [27], all of whom applied integrated power and heat dispatch optimization models, including structural TES in buildings and in the case of Gu et al. [26] and Li et al. [27], also included the heat capacity of the DH piping network. These studies have reported positive effects of TES on DH systems in terms of higher shares of wind power generation (increased generation, lower curtailment rates) and reduced total operational cost of the studied heat and power systems, as compared to the reference systems without TES. Dominkovic et al. [28] have proposed a two-level modeling approach for the analysis of building performance and DR potential of single-family houses coupled with DH. The approach is based on a detailed single-zone simulation model of existing building archetypes, with the objective of estimating their thermal autonomy, i.e., "the time during which the building can perform without activating a heating system", followed by a linear optimization model of the energy system (which includes the power, heat, gas, and transport sectors). The authors observed a reduction in the operational cost of the investigated DH system in the range of 0.7–4.6% when the structural TES in buildings was utilized. Furthermore, the scenario results for 2029 showed that greater benefits could be derived by utilizing structural TES in buildings for the DH system, as compared to the current system composition, owing to the large capacities of the integrated intermittent energy sources.

　　Whereas most of the abovementioned studies have focused on the DR in buildings with electric space heating and on the benefits of building flexibility into the power sector, few studies have investigated the potential of the DR from space heating in buildings connected to DH systems. Furthermore, no studies have provided the possibility to explicitly determine the space heating demand from buildings based on the buildings' physical properties, while taking into account the technical and economic parameters of the DH system, i.e., explicitly accounting for the feedback mechanism between demand and supply. There is also a gap in current knowledge regarding how space heating DR is influenced by the composition of the building stock. To fill this gap, the present work develops a methodology that describes the building stock from a regional perspective, i.e., the city level, with representative buildings, and integrates a building physics energy balance model into a unit commitment, heat generation optimization model of a DH system, thereby hard-linking the energy demand and supply models. Applying the developed modeling methodology, the present study investigates the potential effects of the DR from space heating demand in buildings on the total heating demand and the operation of the DH system. More specifically, we address the following research questions: (1) Which type of DR behavior is induced if flexible space heating is governed by a least-cost operational strategy from a DH system perspective?; (2) What is the potential effect of DR on the total heating demand of buildings and of a city?; (3) Which building type-specific changes are induced by DR in terms of heating and the indoor temperature profiles?; and (4) What would be the impact on the heat generation in the DH system?

　　This paper is organized as follows. Section 2 outlines the modeling approach applied and the case study investigated in this work. Section 3 describes the results obtained from the modeling, and these are further discussed in Section 4. Section 5 summarizes the conclusions drawn from the study.

## 2. Methodology

### 2.1. Modeling Approach

　　The methodology developed and applied in this work builds on previous work by the authors in integrating two separate optimization models: (i) A physical space heating demand model of a BS, which is based on the Energy Carbon and Cost Assessment of Building Stocks (ECCABS) model developed by Mata et al. [29] and further refined by Nyholm [30]; and (ii) a dynamic unit commitment

model of a DH system, as developed by Romanchenko et al. [31]. The outcome of this model integration is a newly created model of the present work, which is termed the Energy Balance Unit Commitment (EBUC) model. EBUC estimates the space heating demand from buildings and calculates the optimal dispatch of heat generation units in a DH system within a single optimization framework. Thus, constraints, which are formulated to estimate the space heating demand in buildings in Reference [30], are refined and added to the formulation of the unit commitment model of a DH system described in Reference [31] to form a part of the total system heating load, as described below. Furthermore, demand response from the space heating in the buildings is enabled by allowing for deviations in the indoor temperature of the buildings, i.e., variations within a predefined temperature span are allowed rather than using a fixed set-point temperature. As a result, the space heating demand in the buildings can be shifted in time as long as the indoor air temperature stays within the pre-defined temperature range. A schematic overview of the EBUC modeling approach is presented in Figure 1.
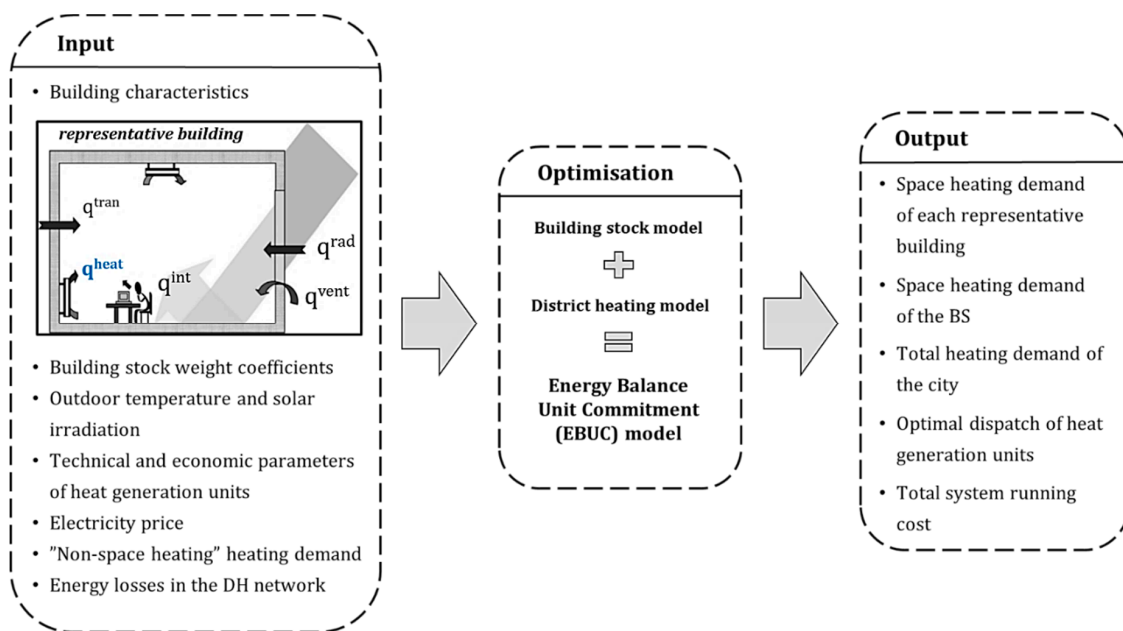


**Figure 1.** Overview of the modeling approach used in this work.

The objective function of the EBUC model is to minimize the total yearly running cost of a DH system, which comprises fuel costs, operation and maintenance costs, and energy and carbon dioxide taxes. The EBUC model is a mixed-integer linear optimization (MILP) model with a time horizon of 1 year and a time resolution of 1 h. The hourly time resolution is chosen to capture short-term heating demand variations and system reactions to changes in hourly electricity prices. The model ensures that in each time-step the level of heat generation is greater than or equal to the total system heating demand, which generally comprises the space heating and hot-water demands from the connected BS, the heating demand from industrial users (if present), and the distribution and conversion losses inherent in the DH network.

### 2.1.1. Modeling the Space Heating Demand in Buildings

The space heating demand in the EBUC model is calculated using an energy balance over each modeled building, while considering two thermal zones. Thus, each building is represented by one external thermal zone, the building envelope, and one internal thermal zone, the indoor air, furniture, and outer layers of internal walls. The calculated space heating demand of each modeled building is then extrapolated to represent the overall space heating demand of the BS using building stock weight coefficients.

The space heating demand is calculated with assumptions made regarding the physical properties of buildings (building stock representation), outdoor climate conditions, and internal heat gains, which are based on activities, such as the work of ventilation fans, lighting, electrical appliances, and occupants (activities are aggregated into the "q$^{int}$" component in Figure 1). Table 1 provides a list of all the parameters included in the modeling. Wind conditions and outdoor air humidity are not included in the energy balance calculations in the present work. Eventual space cooling demand is not included in the optimization.

**Table 1.** The Energy Balance Unit Commitment (EBUC) model input parameters used to characterize the investigated building stock and the investigated district heating system of Gothenburg.

| Building Stock Model | | District Heating Model | |
| --- | --- | --- | --- |
| Description | Units | Description | Units |
| Total heated floor area of a building | m$^2$ | Max/min output limits of a heat generation unit | kWh/h |
| Total area of the external surfaces of a building | m$^2$ | Ramp limits of a heat generation unit | kWh/h |
| Total area of the window surfaces of a building | m$^2$ | Minimum up- and down-times of a heat generation unit | h |
| Shading coefficient of windows | - | Efficiency of a heat generation unit | % |
| Frame coefficient of windows | - | COP value for HPs | - |
| Coefficient of solar transmission through windows | - | Power-to-heat ratio of CHP plants | - |
| Average U-value of a building | kW/m$^2$°C | Fuel cost for a heat generation unit | EUR/kWh |
| Thermal mass of the external thermal zone | kWh/°C | Variable O&M cost of a heat generation unit | EUR /kWh |
| Thermal mass of the internal thermal zone | kWh/°C | Energy tax | EUR /kWh |
| Solar irradiation | kW/m$^2$ | Carbon dioxide tax | EUR /tCO$_2$ |
| Outdoor temperature | °C | Price of Electricity Certificates | EUR /kWh |
| Average constant values of the heat gains due to:<br>- ventilation fan operation, lighting, electrical appliances and occupants | kW/m$^2$ | Start-up cost of a heat generation unit | EUR |
| Hourly profiles of the heat gains due to:<br>- lighting, electrical appliances and occupants | - | | |
| Efficiency of a heat recovery system (if available) | % | | |

When studying the potential of space heating DR in buildings, while allowing for indoor air temperature deviations within a predefined temperature span in the buildings, a simplified assumption is made that the temperature can only increase above the set-point requirement. This makes the implementation of DR within the cost-minimizing EBUC model simple and computationally undemanding. If the temperature constraint was to be relaxed, i.e., both upwards and downwards temperature deviations were allowed, the cost-minimizing model would obviously exploit the possibility to decrease the heat supply, and thereby, the total system running cost. In reality, the implementation of the temperature control might instead consider a penalty cost for the deviation from the set-point temperature, which could be calibrated depending on the level of comfort required, as well as the levels of costs/savings. However, since any sustained downregulation of the temperature is akin to an energy-saving measure, and the focus in the present work is on the DR potential, a simplistic representation of DR with the aid of increased temperature is applied. Additionally, in

reality, indoor temperatures higher than the required set-point temperature usually prevail [32], and hence allowing for only upwards temperature deviations is considered a fair approximation of a real case. It is therefore likely that consumers will find a certain elevation in acceptable indoor temperature, whereas a decreased indoor temperature will most likely be associated with reduced comfort.

### 2.1.2. Finding the Optimal Dispatch of Heat Generation Units

The total system heating demand, which consists of the endogenously calculated space heating demand from buildings and the exogenously supplied non-space heating demand and energy losses in the DH network (piping grid), is in the EBUC model met by the heat generation units available in the investigated DH system. Thus, the assumption is made that the total system heating demand corresponds to the aggregated heat output from the heat generation units (however, as indicated earlier, excess generation of heat is allowed in the modeling if it results in minimization of the total system cost). The model identifies the optimal unit commitment and dispatch of the supply units taking the interactions with the wholesale electricity market into account (which are not explicitly modeled within this work), via CHP plants and HPs. No options for investments in new heat generation technologies are included in the model. The description of the investigated DH system is limited to the technical and economic parameters of the available heat generation units; no characteristics of the DH network are considered, such as potential congestions in the network or any fluid mechanics limitations. The model has perfect foresight and all the model parameters, including hourly outdoor temperatures, solar irradiation values, electricity prices, and fuel costs, are exogenously provided to the model.

### 2.2. Case Study

### 2.2.1. Building Stock of Gothenburg

In this work, 134 representative buildings represent the BS connected to the DH system of Gothenburg, Sweden, which is presented as a case study. The modeled BS comprises single-family dwellings (SFDs), multi-family dwellings (MFDs), and non-residential buildings (NRBs).

The description of the BS of Gothenburg in the model is based on the BETSI (Byggnader Energi, Tekniska Status och Inomhusmiljö) database [33]. The BETSI database contains detailed descriptions of 1800 existing buildings (1400 residential and 400 non-residential), which were chosen by Boverket [34] and Statistics Sweden [35] as being representative of the standing Swedish BS in 2005 (the BETSI study is still considered the most comprehensive characterization of the Swedish buildings, given that it is based on actual measurements for each of the 1800 buildings). By matching the locations of the sample buildings to the location of the city of Gothenburg and by choosing buildings that are indicated as being connected to DH, 27 SFDs and 65 MFDs are extracted from BETSI to represent the residential BS of Gothenburg in 2005. Since 2012 is chosen for the modeling in the present work (due to the availability of data on the investigated BS and DH), one archetype SFD and one archetype MFD are created to represent the buildings constructed under the period 2005–2012. Parameters describing the SFD and MFD archetypes are averaged from the values describing the sample buildings built during the period of 2000–2005, since the building codes for those periods are assumed to be similar. It should be noted that archetype buildings are hypothetical buildings defined for the modeling purposes of this work, while the buildings described in the BETSI database are sample (existing) buildings. Both sample and archetype buildings are used to describe the BS of Gothenburg in this work, and together they will be referred to as 'representative buildings'.

The non-residential BS of Gothenburg is represented by 40 archetype NRBs. This number is obtained by having one archetype building for each building type in each construction period indicated in Table 2. The building types and construction periods were originally identified by the Swedish Energy Agency [36]. For this work, the building types are further aggregated (from the original 13 types) into five types based on the aggregations used in the BETSI report [37].

**Table 2.** The building types and construction periods used to obtain archetype NRBs, which represent the non-residential BS of Gothenburg, i.e., each building type exists for each period, yielding a total of 40 NRB building types.

| Building Type | Construction Period |
|---|---|
| | −1940 |
| 1. Hotels, restaurants, office/administration, food | 1941–1960 |
| commerce, other commercial | 1961–1970 |
| 2. Healthcare 24/7, other healthcare | 1971–1980 |
| 3. Educational | 1981–1990 |
| 4. Dwellings*, religious, garages | 1991–2000 |
| 5. Sports centers, cultural, other | 2001–2010 |
| | 2010– |

* Apartment buildings in which the majority of the area is used for non-residential purposes.

The complete set of parameters describing the representative buildings and the BS weight coefficients applied to these buildings can be found in the Supplementary Materials. New or modified (not extracted directly from BETSI) parameters are explained in Appendix A.

### 2.2.2. "Non-Space" Heating Demand and Energy Losses in the District Heating System of Gothenburg

The hourly values for the energy losses from the DH network are estimated by multiplying an assumed heat loss coefficient of the network by the hourly values of the temperature difference between the mean network temperature and the ground temperature. In this work, the hourly values of the supply and return water temperatures, as well as the heat loss coefficient of the network, which is derived from the information on the total yearly energy losses from the DH network of Gothenburg in 2012 (for further details *cf.* [38]), are provided by the DH operator. The energy transfer losses in the heat exchangers at the substation level of the DH system are assumed to be 10% [39].

The hot-water demand from buildings and the demand from industrial users are assumed to be inflexible demands, and they are supplied to the model exogenously as a single "non-space heating" demand profile. The non-space heating demand profile during the summer season is obtained by subtracting the calculated values of the energy losses in the DH network from the real-life measured total system heating demand (assuming that the space heating demand during the summer period is zero). The non-space heating demand profiles for other seasons are approximated by taking the hourly heat demand profile from one summer month (in this study, the profile from July was chosen) and multiplying it by seasonal correction factors, which represent seasonal variations of the non-space heating demand. The applied seasonal correction factors are estimated to make the average non-space heating demand during the autumn and spring seasons equal to the yearly average non-space heating demand, while the values for the average non-space heating demand during the winter and summer seasons will be 30% higher and 30% lower, respectively, than the yearly average value. This simplification is based on the study of Aronsson [40] and on the assumption that the share of industrial demand is considerably smaller than the share of the hot-water demand in the non-space heating demand (which was observed by comparing the estimated hot-water demand in buildings, based on the model results, and the measured industrial demand in the system).

### 2.2.3. Heat Supply in the District Heating System of Gothenburg

The DH system of Gothenburg is the second largest DH system in Sweden, with a total annual delivery of 3300 GWh of heat to consumers in 2015 [41]. In this work, the DH system is represented by 13 aggregated heat generation units, including CHP plants, heat-only boilers (HOB), and HPs, with the base load being covered by the waste heat from two refineries and a municipal waste incineration plant. Assumptions regarding the technical and economic parameters that describe the heat generation units investigated in this work (listed in Table 1) can be found in Appendix B and elsewhere [31,42]. The

hourly values for the supply and return water temperatures in the DH network were provided by the DH system operator. This work applies the existing generation fleet of the DH system of Gothenburg, which means that investments in new generation capacities are not considered. Interconnections of the modeled DH system with the DH systems of the neighboring municipalities are not modeled in this work, as the transfers are small.

### 2.2.4. Other Input Data

The hourly outdoor air and ground temperatures for 2012 are provided by the DH system operator. The solar irradiation data are obtained from the SMHI (Swedish Meteorological and Hydrological Institute) [43]. The hourly day-ahead electricity spot prices are taken from the Nordic electricity market "Nordpool" [44]. The fuel prices for heat generation units are obtained from the Swedish Energy Agency [45], except for bio oil and natural gas, the prices of which are assumed from the data in purchase contracts. The energy and carbon taxes are taken from Nordenergi WG [46]. The price for Electricity Certificates, which support renewable electricity generation in Nordic countries, is provided by the Swedish Energy Agency [47].

### 2.3. Investigated Scenarios

To study the potential of space heating DR in buildings, three scenarios with different allowances in relation to indoor temperature variations are investigated. In the Reference scenario, no DR is allowed in the investigated buildings, i.e., the space heating demand is calculated with the objective of maintaining the indoor set-point air temperature in the buildings at a fixed value. However, the indoor air temperature is not prevented from rising above the set-point value due to the influences of the outdoor air temperature, solar irradiation, or internal heat gains. The set-point air temperatures for SFDs and MFDs are 21.4 °C and 22.5 °C, respectively, based on the values for the mean indoor temperatures in Swedish households reported in the study of Langer and Bekö [32]. The set-point indoor air temperature for NRBs is 20 °C, based on the data available from Grundsell [48]. In the DR 1 °C and DR 3 °C scenarios, space heating DR is allowed. The DR is achieved through the possibility to increase the indoor air temperature of the investigated buildings above the set-point air temperature by 1 °C and 3 °C, respectively. Resulting temperature spans of 1 °C and 3 °C are compatible with the recommended indoor temperature comfort ranges of 21 °C–25 °C for living spaces (according to ISO standard for Ergonomics of the Thermal Environment [49]) and 20 °C–24 °C (winter, warm clothing) and 23 °C–25.5 °C (summer, light clothing) for office environments (drawn from the research and calculations by American Society of Heating and Refrigerating and Air Conditioning Engineers (ASHRAE) [50]).

## 3. Results

### 3.1. Model Validation

Figure 2 shows a comparison of the measured total heat generation (as given by the local DH system operator) and the corresponding modeled results for February and March of 2012 (the year studied). It should be borne in mind that the modeled total system heating demand is the sum of the exogenously provided data on the non-space heating demand and the energy losses in the DH network, whereas the space heating demand from buildings is calculated in the model. The real-world measurements differ from the modeling results in two ways:

- the modeled total heat generation is lower than the measured generation,
- the modeled heat generation profile fluctuates more than the measured profile.
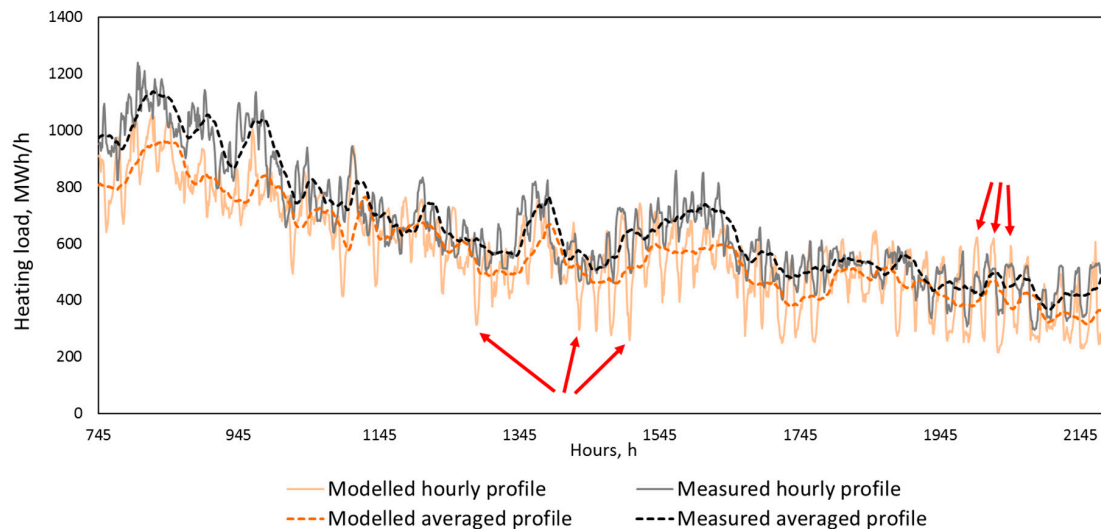
**Figure 2.** The measured and modeled heat generation profiles of the investigated DH system of the City of Gothenburg presented for February and March of 2012. The daily averaged profiles are obtained by applying the moving average function with the 24 h interval to the original hourly profiles. The red arrows mark pronounced variations in the modeled heat generation profile.

The model results reveal 3.2 TWh of heat generated in Year 2012, which is 9% lower than the measured total system heating generation during that year (summer months are excluded from the modeling and comparison, as the space heating demand during those months is zero). Furthermore, the difference between the modeled and measured generation during the winter season is greater than that during the autumn/spring period, i.e., 12% versus 6%, respectively. Possible reasons for the identified differences between the modeled and measured generation are: (a) underestimation of the non-space heating demand in the modeling, e.g., demand for space heating from industry, especially during the colder part of the year; (b) overestimation of the U-values for the investigated buildings, and consequently, underestimation of the energy losses from the buildings; and (c) the fact that the indoor air temperatures in buildings exhibit significant variations (due to poor heat control systems [51]) and are often higher than the modeled set-point value.

Figure 2 shows that the modeled heat generation profile exhibits more pronounced variations, i.e., fluctuates to a greater extent, as compared to the measured data. This behavior is especially pronounced during the spring and autumn seasons. The most likely reasons for the variations in the heat generation profiles are: (1) The impacts of outdoor humidity and wind conditions, which are not included in the model, on the space heating demand; (2) overestimation in the model of the heat gains through windows due to solar irradiation, which is of higher intensity in the spring/autumn period; (3) the utilization of the inherent thermal storage potential of the DH piping network by the DH system operator, which is not included in the modeling but is used in reality; and (4) the fact that owing to poor heat control systems, buildings are occasionally supplied with more heat from DH systems than they require in reality, which leads to increases in the indoor temperature and/or the opening of windows for cooling.

While the above differences between the modeled and measured heat generation data render the model unsuitable for precise quantitative predictions, the model should be appropriate for the purpose of this work, i.e., to study the potential of the space heating DR of the investigated BS on the DH system.

### 3.2. Peak Shaving and Valley Filling of the Total System Heating Demand

The results from the modeling show that the space heating DR in buildings can significantly affect the total system heating demand of the city by smoothening its variations. From Figure 3, it is clear that there are periods during which the heat generation in the DR 3 °C scenario exceeds the heat generation in the Reference scenario (exemplified in Figure 3 as valley filling). Thus, the indoor temperature of the investigated multi-family houses increases, i.e., the thermal energy is stored. Likewise, there are periods when the heat generation is lower than the demand. During these periods, the stored thermal energy from the previous over-heating periods is used, and the indoor temperature of the buildings decreases simultaneously (exemplified in Figure 3 as peak shaving).
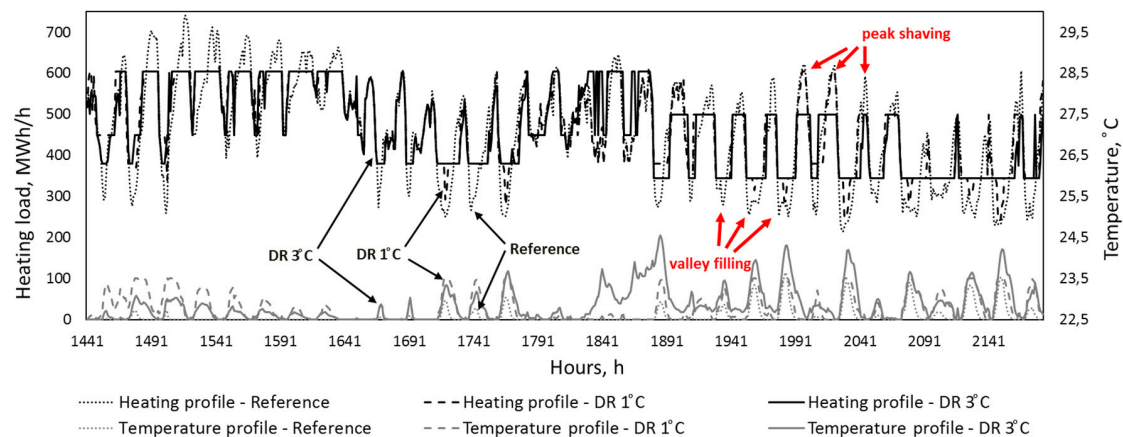


**Figure 3.** Heating demands of the DH system of the City of Gothenburg and the average indoor air temperatures in the representative multi-family houses that were investigated, as obtained through EBUC modeling for March 2012 in the Reference, DR 1 °C, and DR 3 °C scenarios.

The total shifted space heating demands over the modeled period in the DR 1 °C and DR 3 °C scenarios were 194 GWh and 226 GWh, respectively, as compared to the Reference scenario. These values correspond to 6.1% and 7.1%, respectively, of the total yearly system demand in the Reference scenario. The maximum space heating demand shifted for the purpose of peak shaving, which occurred in the DR 3 °C scenario, was 213 MWh/h, which corresponds to 25% of the heating demand during that hour in the Reference scenario. The highest value for the shifted demand for valley filling was 241 MWh/h, which also occurred in the DR 3 °C scenario. The corresponding values for demand shifting for peak shaving and valley filling in the DR 1 °C scenario were 207 MWh/h and 219 MWh/h, respectively. These results indicate diminishing returns in relation to the potentials for valley filling and peak shaving in the case of DR 3 °C over-heating, as compared to DR 1 °C over-heating. Moreover, as indicated above (cf. [49,50]), it can be assumed that 1 °C indoor temperature variations are acceptable to the inhabitants in contrast to the 3 °C variations, which are likely to require additional incentives to become accepted.

### 3.3. Effects of Demand Response on the System Heat Demand Variations

The extent to which the total system heating demand was smoothened due to the active space heating DR in buildings was characterized using the indicator Relative Daily Load Variations (RDLVs, further explained in Appendix C) presented in Figure 4. The results show that the DR 3 °C scenario smoothens the daily heat demand variations in the investigated DH system to a greater extent than the DR 1 °C scenario does, giving decreases of 31% and 18%, respectively, as compared to the Reference scenario.
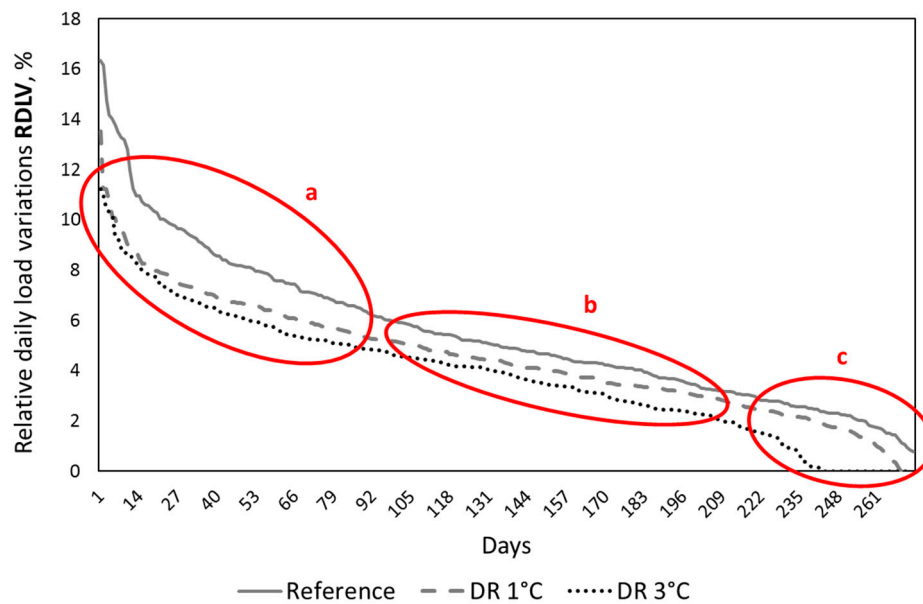
**Figure 4.** The Relative Daily Load Variations (RDLVs), sorted in descending order, for the investigated DH system of the City of Gothenburg, as obtained from the modeling for the Reference, DR 1 °C, and DR 3 °C scenarios. Note that the modeled period is limited to 273 days, excluding the summer months, during which no space heating demand, and respectively, no DR are present.

The results show that the largest daily heat demand variations in all the investigated scenarios primarily occur during the spring-autumn months of the year, with most of the days lying within area **a** of Figure 4. During the winter months, the heat demand variations are lower, such that most of the winter days are within area **b** of Figure 4. Such seasonal differences in daily heat demand variations can be explained by pronounced fluctuations in the daily outdoor temperatures and stronger solar irradiation during the spring-autumn seasons of the year, as compared to winter.

In Figure 4, it is evident that the DRs obtained through over-heating of the buildings by both 1 °C and 3 °C decrease the heat demand variations to a similar extent; this is true for both areas **a** and **b** of Figure 4. However, in area **b** (mainly, the winter period), the DR of the buildings has a weaker effect on the heat demand variations. This is mainly due to a greater DR potential of buildings during the spring/autumn period than during the winter period, i.e., the stored thermal energy during the spring/autumn period can be spread out over a longer time period due to lower energy losses from the buildings. In addition, high demand calls for the dispatch of peaking heat generation units. Storing thermal energy in buildings can delay (and sometimes prevent) the use of peaking units, although high energy losses from buildings, and thus, short storage times will still require the starting up of such peaking heat generation units. Since these units are designed to adjust their outputs according to short-term heat demand fluctuations (easy to start up and adjust the output), it is less beneficial to activate DR in the buildings. Meanwhile, during the spring/autumn period, the heating demand is at a level at which mid-load units can cover the whole demand more often, so that the operation of peaking HOBs can be avoided.

Area **c** in Figure 4 indicates that the space heating DR in the DR 3 °C scenario has a sufficiently high capacity to completely smoothen some of the intraday heat demand variations. This result is also evident in Figure 3, where the heat demand remains at 330 MWh/h for a significant period of time, with the maximum period being almost two consecutive days. This constant heating demand means that the generation of heat can be optimized more easily and scheduled to ensure the best economic and/or environmental performance (if other influential parameters, e.g., electricity price, vary insignificantly). In the investigated DH system of Gothenburg, 330 MWh/h of heat is the aggregated output of the waste-heat technologies, i.e., technologies that make use of the waste heat from industries and municipal waste incineration. Thus, the space heating DR obtained by allowing +3 °C indoor

temperature deviations in the buildings connected to the DH system has the potential to increase the number of hours during which all the heat delivered to the customers in the city is generated from heating energy that would otherwise be wasted. One should remember that this is the case-specific result for the city of Gothenburg and that the modeled system heating demand is slightly lower than the measured demand (as indicated in Section 3.1). However, the results show that the DR potential in buildings has not reached its limit, i.e., not all the buildings were overheated by 3 °C during the hours of flattened demand.

### 3.4. Effect of Demand Response on the Studied Building Stock

The results from the modeling show that allowing for active DR affects both the total demand and the profile of space heating demand in the investigated buildings. The total yearly space heating demand of the investigated BS increases (since only increase in the indoor temperature is allowed) by 2.8% and 2% in the DR 1 °C and DR 3 °C scenarios, respectively, as compared to the Reference scenarios. The results also show that the total space heating demand of the investigated BS is distributed between the building types as follows: 12% from SFDs; 68% from MFDs; and 20% from NRBs.

Figure 5 shows the duration curves for the charge and discharge rates of the SFDs, MFDs, and NRBs, as obtained from the modeling for the Reference and DR 3 °C scenarios. "Charging" of buildings is defined as the hours during which the values of the space heating demand are higher than the corresponding values in the Reference scenario (more heat is supplied to the buildings than is required). Correspondingly, the "discharging" of buildings occurs during the hours when space heating demand is lower than in the Reference scenario (less heat is supplied than required). The results show that the charging of buildings, regardless of the type of building, occurs at higher rates than does the discharging of buildings. Furthermore, the modeling shows that the total yearly amount of heat supplied through charging of the BS is 36% larger than the amount of heat undersupplied during discharging (total discharged energy). This indicates that more than one-third of the thermal energy stored in buildings is lost in the form of increased losses. The duration curves for the charging and discharging of buildings in the DR 1 °C scenario follow trajectories similar to those in the DR 3 °C scenario, although both the charging and discharging occur at lower rates.
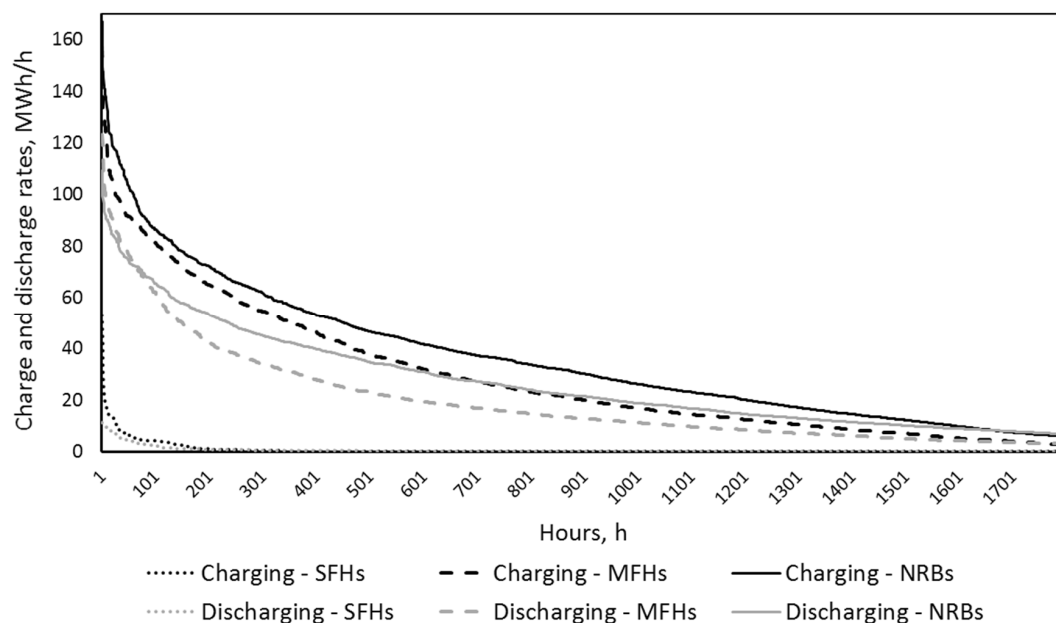


**Figure 5.** Duration curves for the hourly charging and discharging rates obtained from the modeling of the SFDs, MFDs, and NRBs connected to the DH system of the City of Gothenburg, for the Reference and DR 3 °C scenarios. Note that the x-axis only extends to 1800 h (during the remaining hours, the values are low, and thus, are not shown).

Figure 6 shows the hourly profiles of the specific heating demands of the SFDs, MFDs, and NRBs for 3 days in February, March and May in the Reference, DR 1 °C, and DR 3 °C scenarios. The days are chosen to represent periods with cold, moderate, and warmer outdoor temperatures. The results indicate that the specific heating demand of the investigated SFDs is greater than the specific heating demands of the MFDs and NRBs, regardless of the outdoor air temperature (time of the year). It is also clear that, during the colder periods of the year, the NRBs take part in DR more actively than do the SFDs and MFDs. During the warmer periods of the year, all the building types are active in DR. It is also evident that, with DR, the amplitude between the peaks and dips in the profiles of the SFDs and MFDs decreases, i.e., the profiles become flatter, while for NRBs, this amplitude increases, as compared to the profile obtained for the Reference scenario. This (together with results from Figure 5) indicates that the space heating demand of NRBs is being adjusted to a greater extent than the demand of the residential BS. Together with the fact that the total yearly space heating demand from the NRBs is 3.5-times lower than that from the MFDs, this indicates that the NRBs are prioritized over the residential BS for DR. These results can be explained as reflecting that the specific thermal masses of the NRBs are on average larger, while the U-values are lower than those of the SFDs and MFDs. This means that the NRBs have a higher thermal energy storage capacity and lower energy losses than the SFDs and MFDs, and thus, are activated for DR more than the other building types. However, it should be noted that the NRBs used in the present work are archetype buildings, while the residential BS is described using sample (existing) buildings. This means that the uncertainty surrounding the description of NRBs, and thus, the uncertainty regarding the potential for DR from NRBs are more pronounced than the uncertainties related to the MFDs and SFDs.

The modeling results show that as a result of DR, the indoor air temperature of buildings can continuously fluctuate for a couple of days at levels higher than the set-point temperature (periods when thermal energy is stored). Whereas the durations of periods of continuous increase (charging) and decrease (discharging) of the indoor temperature never exceeds 24 h.

*3.5. Effect of Demand Response on Heat Generation*

The smoothening of the total heating demand of the DH system provided by the flexible space heating demand in buildings has a significant impact on heat generation in the DH system. The main impacts of the DR on the operation of the DH system are increased heat supply from the base-load units and decreased heat generation from peaking HOBs.
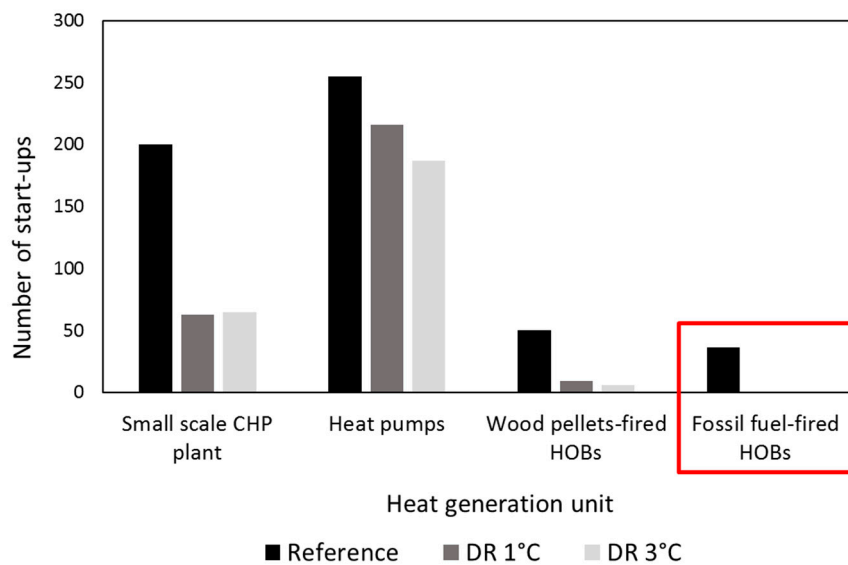
Figure 7 shows the numbers of start-ups for the small-scale, gas-fired CHP plant, the HPs, and the peaking HOBs fueled by wood pellets or fossil fuels. The results indicate that allowing the indoor temperature in buildings to increase by just 1 °C (the DR 1 °C scenario) results in a significant drop in the number of start-ups required for the heat generation units. Furthermore, it is evident that increasing the allowed indoor-temperature deviations by up to 3 °C (the DR 3 °C scenario) has little additional impact on the number of start-ups, as compared to the allowed 1 °C deviations. Peaking HOBs are affected the most in terms of the number of start-ups, which are reduced by more than 80% for the wood-fired HOBs, whereas the use of fossil fuel-fired HOBs can be avoided entirely in both the DR 1 °C and DR 3 °C scenarios, as compared to the Reference scenario.
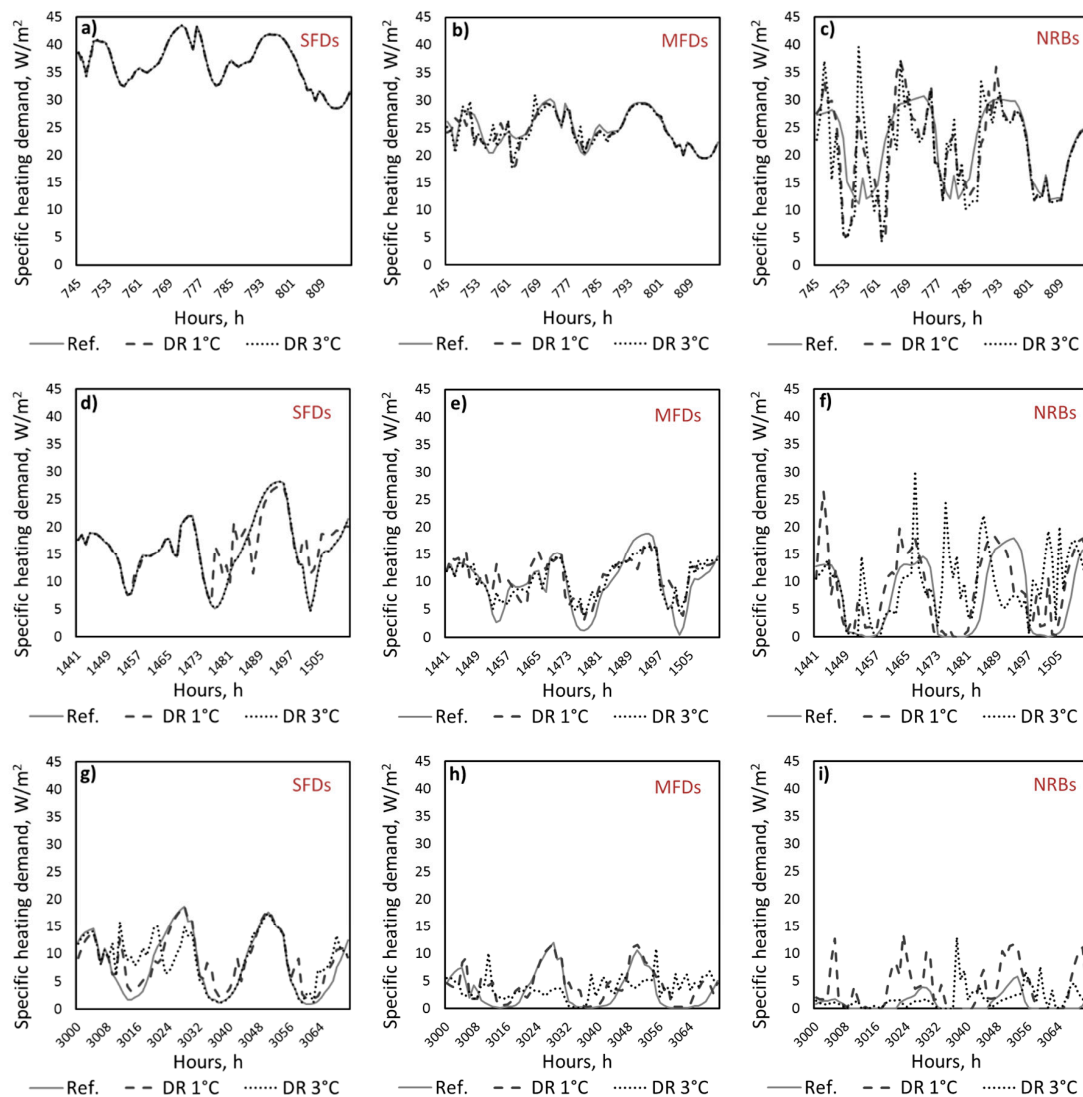
**Figure 6.** Specific (W/m$^2$) hourly heating demand profiles of the SFDs, MFDs, and NRBs connected to the DH system of the City of Gothenburg, as obtained from the modeling for the Reference, DR 1 °C, and DR 3 °C scenarios. The profiles are shown for 3 days in: February, with average outdoor temperature of −10.7 °C (**a**–**c**); March, with average outdoor temperature of 3.8 °C (**d**–**f**); and May, with average outdoor temperature of 7 °C (**g**–**i**), all in 2012.

The results show that the utilization rate of the waste-heat technologies increases in the scenarios with DR, as compared to the Reference scenario. Considering that, in all the investigated scenarios, the waste-heat technologies supply around 65% (just above 2000 GWh) of the total system heating demand, the increases in heat supply of 65 GWh and 67 GWh for the DR 1 °C and DR 3 °C scenarios, respectively, as compared to the Reference scenario, are small. Nevertheless, the effect of the increase in heat supply from waste-heat technologies due to DR on the utilization patterns of the dispatchable heat generation units (CHP plants, HPs, and HOBs) is considerable, with the actual number of hours of operation being reduced significantly. This enables a higher percentage of the operation to be conducted at levels close to the rated capacities of the units, as compared to the Reference scenario without DR.

**Figure 7.** Numbers of start-ups for the heat generation units in the DH system of the City of Gothenburg, as obtained from the modeling for 2012 for the Reference, DR 1 °C, and DR 3 °C scenarios.

The operational changes that occur in the DH system of Gothenburg following the integration of flexible demand into the supply are associated with economic benefits. The modeling results indicate that the total yearly system running costs can be up to 4% and 5% lower in the DR 1 °C and DR 3 °C scenarios, respectively, as compared to those in the Reference scenario. Furthermore, a more-stable operation in combination with fewer start-ups of the heat generation units is likely to ease the control of the DH system from the operator's perspective, and potentially, decrease the wear on the equipment, thereby reducing the need for maintenance and repairs. This will extend the lifespans of the units and lead to even greater savings. Finally, significantly reduced utilization of the peaking HOBs, which at present are mainly gas- and oil-fired, would reduce the environmental footprint of the heat supply of the city.

## 4. Discussion

The modeling carried out in this work is based on the method for assessing the DR potential from space heating demand in buildings by allowing exclusively for upward variations from a set-point indoor temperature. However, other methods can be used to assess the energy flexibility of buildings, as reviewed by Lopes et al. [52]. One such method, which allows for both downward and upward variations of the temperature around the set-point temperature, while having a penalty cost that depends on the degree of the deviation, was applied in the study of Nyholm et al. [25]. They concluded that, for the system investigated (Swedish SFDs in the context of the Northern European electricity system), allowing for both upward and downward temperature variations resulted in greater economic benefit at lower temperature deviations from the set-point temperature, as compared to only allowing for upward deviations, which required large temperature deviations to achieve the same economic benefit.

As indicated in Section 2, the non-space heating demand and energy losses in the DH network are estimated beforehand and exogenously provided to the model in this work. Since the hourly profile for energy losses is based on the measured temperatures of the supply and return water in the DH network and the surrounding ground temperature, it is assumed to be sufficiently accurate for the present work. The estimation of the non-space heating demand profile can be considered to have a greater degree of uncertainty, and to require more detailed data characterizing the industrial heat demand and shares of the space and water heating demands in buildings. Alternatively, hot-water demand in buildings could be explicitly calculated within the model. This would require the collation of substantial statistical information, since hot-water demand in buildings, in contrast to space heating

demand, is mainly dependent upon the preferences and habits of the inhabitants, rather than on the weather conditions. With more low-energy buildings being constructed and connected to DH systems, the share of hot-water demand in the total energy consumption profile of buildings will increase. Thus, further research is needed regarding the possibility to make the hot-water demand controllable, with the objective of contributing to DR from buildings.

The input parameters that describe both the residential and non-residential buildings modeled in this work are based mainly on the detailed measurements from the BETSI study and should give a good representation of the BS of Gothenburg. However, refinement of the following input data could change the DR potential studied in the present work and should be performed in the future: (a) The number and type of identified representative (archetype) non-residential buildings; (b) the building stock weight coefficients defined for the city of Gothenburg by downscaling the national coefficients defined in BETSI; (c) an estimation of the effective heat capacities (thermal masses) of buildings; and (d) the hourly profiles of the internal heat gains.

As this work uses the building stock and the DH system of Gothenburg as a case study, it is influenced by local conditions, in particular that it has a very high share of industrial waste heat and the presence of industrial heat pumps in its generation mix. Thus, the observed economic benefits conferred by active DR in buildings to the investigated DH system, e.g., the reported savings in the total system running cost are also case-specific. Nevertheless, even if the compositions of other DH systems are different there will still be base-load, mid-load, and peaking units, the operation of which will be influenced by the DR from buildings through fewer starts and stops of peaking units and increased utilization of base-load units. In contrast, the shape of the demand duration curve becomes more decisive for the outcomes, in that a system with a more-uniform (flat) demand duration curve will have different characteristics in the cost structure of the production mix, and therefore, will be influenced differently by the DR in buildings. Additionally, the observed benefits from active DR in buildings to the DH system are specific for the method used in this study, i.e., application of an optimization model with perfect foresight. In reality, weather forecasts and electricity price predictions are updated on short-term basis (daily and weekly). Hence, for day-to-day operational strategies of DH systems either the proposed EBUC model in this study can be reformulated, e.g., incorporating a so-called rolling planning horizon approach, or other modeling tools should be used.

## 5. Conclusions

The flexibility potential of DR from space heating demand in buildings for district heating systems is investigated using an integrated demand-supply optimization model that co-optimizes the space heating demand in buildings and the dispatch of heat generation units within the DH system.

The modeling results indicate that space heating DR in buildings has a significant impact on the total heating demand profile of a city by smoothening its fluctuations. The smoothening of fluctuations is achieved through both valley filling and peak shaving. It is clear that the maximum level of demand shifting achievable in the DR 1 °C scenario (allowing for an upwards temperature increase of up to 1°C from the set-point temperature) is almost the same as that in the DR 3 °C scenario, suggesting that the effects of increasing the allowed temperature deviation are marginal. The highest value for the space heating demand shifted, for the purpose of peak shaving, was observed in the DR 3 °C scenario, and reached 25% of the heating demand during that hour in the Reference scenario. The total shifted space heating demand for the entire year was 8.4% in the DR 1 °C scenario and 9.4% in the DR 3 °C scenario, as compared to the total heating demand in the Reference scenario.

The DR from buildings is identified as being most effective during the period when daily heat-demand variations are greatest, i.e., during the spring and autumn months. It is evident that as a result of DR, the indoor air temperature of buildings can continuously fluctuate at levels higher than the set-point temperature (periods when thermal energy is stored), and correspondingly, change the space heating demand profile during a couple of days. Yet, the durations of periods of continuous increase (charging) and decrease (discharging) of the indoor temperature never exceed 24 h. The

results also show that the charging of buildings occurs at higher rates than does the discharging of buildings. In addition, the results indicate that, in the investigated building stock, non-residential buildings are used for DR more actively than residential buildings.

The results show that flattening the total system heating demand results in more-efficient heat generation. We show that the heat supply from base-load units increases, while the output from peaking HOBs decreases in the scenarios that allow DR. Our results reveal that the DR achieved through over-heating of buildings by just +1 °C leads to dramatic reductions in the numbers of starts and stops of peaking units. As examples, a decrease of more than 80% is registered for wood pellet-fired units and there is a 100% decrease for all fossil-fired heat-only boilers. These results imply that the available peaking capacities can be used less frequently, and therefore, some of them can be retired. Thus, costly investments in new peaking units can be avoided in the future if DR is applied. Following the changes made to the heat generation strategies, we also observe a decrease in the total running cost of the investigated DH system, with the largest reduction of 5% appearing in the DR 3 °C scenario, as compared to the current mode of system operation.

## Appendix A

The national BS weight coefficients used to scale up the representative MFDs and SFDs to the total residential BS of Sweden are extracted from BETSI. The data for the year of construction (available in [35]) and for the number of residential buildings connected to the DH system of Gothenburg (90% of MFDs and 20% of SFDs, as indicated by the DH system operator [42]) are used to recalculate the national BS weight coefficients of MFDs and SFDs, so as to represent the residential BS of Gothenburg in this work. The total heated floor area of MFDs estimated in this work is also verified against the data from the study of Mangold et al. [53]. In total, 9700 SFDs and 5300 MFDs with total heated floor areas of 1.5 mln m$^2$ and 15.8 mln m$^2$, respectively, represent the residential BS of Gothenburg connected to the city's DH system in the modeling of this work.

The national BS weight coefficients for NRBs are derived from the available statistics on the total number and the total heated floor area of NRBs in Sweden, as published by the Swedish Energy Agency [36]. The data on the total heated floor area of NRBs located in the Västra Götaland region, the region in which Gothenburg is located, and the numbers of residents living in the region and in the city are used to recalculate (downscale in this case) the national BS weight coefficients to the coefficients that are applied to the non-residential BS of Gothenburg. The assumption is made that all NRBs available in the city are connected to DH. As a result, 3600 NRBs with a total heated floor area of 6.2 mln m$^2$ are modeled in this work.

The values for the total heated floor area, total area of external surfaces and windows, and average U-value (*cf.* Table 1) for archetype NRBs identified in this work are obtained by modifying the data from BETSI as follows:

For building types 1, 2 and 5 (*cf.* Table 2), the values are obtained by performing the following manipulations (total heated floor area is taken as an example): (1) the heated floor area of each sample building, belonging to one of the types described in BETSI, is multiplied by the respective BS weight

coefficient; (2) the values obtained in step 1 for all the sample buildings within each building type and construction period are summed; and (3) the sum obtained in step 2 is divided by the sum of the BS weight coefficients applied to all sample buildings within each respective building type and construction period. The obtained values for the total heated floor area are applied as the total heated floor areas of the archetype NRBs identified in this work.

Owing to a lack of data in BETSI, the total heated floor area for the NRBs of building types 3 and 4 (*cf.* Table 2) is estimated by dividing the total heated floor area of all buildings of the same building type and construction period (obtained by downscaling the national values of the total heated floor area from the Swedish Energy Agency [36] using the statistics on the number of buildings in the Västra Götaland region and in Gothenburg) by the respective BS weight coefficients. The values of the external surfaces of buildings and windows for the NRBs of building types 3 and 4 are calculated by multiplying the estimated values of the total heated floor area by the proportions between the total heated floor area and external and window surface areas of buildings estimated based on the data from the Swedish Energy Agency [36] and Boverket [34].

U-values for the NRBs of building type 3 are obtained from the study of Grundsell [48]. Due to the lack of data, the U-values for NRBs of building type 4 are derived by taking an average of the U-values for the NRBs of other building types from the corresponding construction periods.

The thermal mass of the external thermal zone of the SFDs is calculated by multiplying the specific heat capacity per unit of floor area (derived from Hedbrant [54]) by the total heated floor area of the building. For MFDs and NRBs, the thermal mass of the external thermal zone is the sum of the volumetric heat capacities of the components of the building envelope, i.e., the walls, roof, floors, and windows. The volumetric heat capacity of each component of the building envelope is calculated by multiplying the density, specific heat capacity, surface area and thickness of each component (*cf.* [48]). The thermal mass of the internal thermal zone of each building is estimated based on the findings of Hedbrant [54]: it is assumed that the ratio of the thermal masses of the external and internal thermal zones in "heavy" buildings (buildings built from concrete, bricks and stones) is 61% to 39%, while in "light" buildings built from, for example, gypsum boards with glass-wool insulation, the proportion is 68% to 32%.

The hourly values for the internal heat gains (lighting, electrical appliances and occupants) in each representative building are calculated by multiplying the annual average internal heat gain values by the hourly heat gain profiles (*cf.* Table 1). The values for the annual average heat gains for MFDs and SFDs are extracted from BETSI. The hourly heat gain profiles for MFDs and SHFs are taken from the study of Nyholm et al. [2]. The values for the annual average heat gains and the hourly heat gain profiles for NRBs are based on the study of Grundsell [48]. Heat gains due to the operation of ventilation fans are assumed to be constant over the modeling period. The data related to the window properties and the ventilation rates (*cf.* Table 1) applied to the NRBs are obtained from the study of Grundsell [48].

## Appendix B

**Table A1.** Parameters of the heat-only boilers (HOBs) and combined heat and power (CHP) generation units available in the district heating system of Gothenburg. The efficiencies of the Sävenäs CHP and the Sävenäs HOB1 units have values higher than "1" because the calculations are performed based on the lower heating value of the fuel (a flue gas condensation technology is used in these units).

| Unit Name | Unit Type | Fuel Type | Total Efficiency/COP | Max/Min Output, MWh/h | Ramp-Up/Ramp-Down Limits, MWh/h | Minimum Up-Time/Down-Time, h | Power-to-Heat Ratio |
|---|---|---|---|---|---|---|---|
| **Heat Generation Capacity** | | | | | | | |
| Oil refinery 1 | - | waste heat | 1 | 85/40 | 22.5 | 8760 | |
| Oil refinery 2 | - | waste heat | 1 | 75/40 | 7.5 | 8760 | |
| Waste Incineration CHP | - | waste heat | 1 | 185/75 | 55 | 8760 | |
| Sävenäs CHP | CHP | wood chips | 1.11 | 105/35 | 35 | 24 (down-time) | |
| RYA CHP | CHP | natural gas | 0.91 | 295/50 | 245 | - | |
| Högsbo CHP | CHP | natural gas | 0.79 | 14/3 | 11 | - | |
| RYA HPs | HP | electricity | 3.45 | 155/30 | 125 | - | |
| RYA HOBs | HOB | wood pellets | 0.9 | 100/25 | 75 | 6(up-time) | |
| Sävenäs HOB 1 | HOB | natural gas | 1.01 | 90/20 | 70 | - | |
| Sävenäs HOB 2 | HOB | natural gas | 0.9 | 60/20 | 40 | - | |
| Rosenlund HOB | HOB | natural gas | 0.9 | 120/30 | 90 | - | |
| Angered HOBs | HOB | bio oil | 0.90 | 100/15 | 85 | - | |
| Rosenlund HOBs | HOB | fuel oil | 0.88 | 300/20 | 280 | - | |
| **Electricity Generation Capacity** | | | | | | | |
| Sävenäs CHP | CHP | wood chips | - | 13/3 | 5 | - | 0.12 |
| RYA CHP | CHP | natural gas | - | 245/41.5 | 203.5 | - | variable |
| Högsbo CHP | CHP | natural gas | - | 13/2.8 | 10 | - | 0.93 |

**Table A2.** Costs and taxes for the heat-only boilers (HOBs) and combined heat and power (CHP) generation units available in the district heating system of Gothenburg.

| Unit Name | Fuel Cost, SEK/MWh | Variable O&M Cost, SEK/MWh | Energy Tax, SEK/MWh | Carbon Dioxide Tax, SEK/tCO$_2$ | Electricity Certificate, SEK/MWh | Start-Up Cost, SEK |
|---|---|---|---|---|---|---|
| Oil refinery 1 | - | 10 | - | - | - | - |
| Oil refinery 2 | - | 10 | - | - | - | - |
| Waste incineration CHP | - | 10 | - | - | - | - |
| Sävenäs CHP | 209 | 87 | - | - | 168 | 200,000 |
| RYA CHP | 230 | 22 | 25 | - | - | 400,000 |
| Högsbo CHP | 230 | 22 | 25 | - | - | - |
| RYA HPs | price profile | 20 | 290 | - | 168 | - |
| RYA HOBs | 292 | 28 | - | - | - | - |
| Sävenäs HOB1 | 230 | 15 | 82 | 950 | - | - |
| Sävenäs HOB2 | 230 | 15 | 82 | 950 | - | - |
| Rosenlund HOB | 230 | 15 | 82 | 950 | - | - |
| Angered HOBs | 600 | 15 | - | - | - | - |
| Rosenlund HOB1 | 542 | 15 | 82 | 950 | - | - |

O&M, Operation and maintenance cost; SEK, Swedish kronor.

The EBUC model is implemented in the modeling language GAMS [55]. The relative optimality gap ("optcr" option) of the optimization problem is set at 0.005, which lies within the range of values applied elsewhere [56,57].

**Appendix C**

Relative daily load variations are defined as follows:

$$Relative\ daily\ load\ variations = \frac{\frac{1}{2} \cdot \sum_{h=1}^{24} |Load_h - Load_d|}{Load_{yr} \cdot 24} \tag{A1}$$

where $Load_h$, $Load_d$, $Load_{yr}$ are the hourly, daily, and yearly average heat loads, respectively. The relative daily load variations, which are defined by Gadd and Werner [58], are determined for each day of the year and represent the amount of heat that is diverted from the daily average heat load.

**References**

1. International Energy Agency (IEA). *Transition to Sustainable Buildings—Strategies and Opportunities to 2050*; International Energy Agency: Paris, France, 2013.
2. Nyholm, E.; Puranik, S.; Mata, E.; Odenberger, M.; Johnsson, F. Demand response potential of electrical space heating in Swedish single-family dwellings. *Build. Environ.* **2016**, *96*, 270–282. [CrossRef]
3. Turker, H.; Bacha, S. Smart Charging of Plug-in Electric Vehicles (PEVs) in Residential Areas: Vehicle-to-Home (V2H) and Vehicle-to-Grid (V2G) concepts. *Int. J. Renew. Energy Res.* **2014**, *4*, 859–871.
4. European Commission. "ec.europa.eu". Available online: https://ec.europa.eu/energy/en/topics/energy-efficiency/heating-and-cooling (accessed on 21 February 2018).
5. Åberg, M. Investigating the impact of heat demand reductions on Swedish district heating production using a set of typical system models. *Appl. Energy* **2014**, *118*, 246–257. [CrossRef]
6. Swedish Energy Agency. *Energy in Sweden 2015*; Swedish Energy Agency: Eskilstuna, Sweden, December 2015.
7. Junker, R.G.; Azar, A.G.; Lopes, R.A.; Lindberg, K.B.; Reynders, G.; Relan, R.; Madsena, H. Characterizing the energy flexibility of buildings and districts. *Appl. Energy* **2018**, *225*, 175–182. [CrossRef]
8. Stinner, S.; Huchtemann, K.; Müller, D. Quantifying the operational flexibility of building energy systems with thermal energy storages. *Appl. Energy* **2016**, *181*, 140–154. [CrossRef]
9. Finck, C.; Li, R.; Kramer, R.; Zeiler, W. Quantifying demand flexibility of power-to-heat and thermal energy storage in the control of building heating systems. *Appl. Energy* **2018**, *209*, 409–425. [CrossRef]
10. Hewitt, N.J. Heat pumps and energy storage—The challenges of implementation. *Appl. Energy* **2012**, *89*, 37–44. [CrossRef]
11. Heier, J.; Bales, C.; Martin, V. Combining thermal energy storage with buildings—A review. *Renew. Sustain. Energy Rev.* **2015**, *42*, 1305–1325. [CrossRef]
12. Arteconi, A.; Hewitt, N.; Polonara, F. State of the art of thermal storage for demand-side management. *Appl. Energy* **2012**, *93*, 371–389. [CrossRef]
13. Reynders, G.; Diriken, J.; Saelens, D. Generic characterization method for energy flexibility: Applied to structural thermal storage in residential buildings. *Appl. Energy* **2017**, *198*, 192–202. [CrossRef]
14. Reyndes, G.; Nuytten, T.; Saelens, D. Potential of structural thermal mass for demand-side management in dwellings. *Build. Environ.* **2013**, *64*, 187–199. [CrossRef]
15. Dreau, J.L.; Heiselberg, P. Energy flexibility of residential buildings using short term heat storage in the thermal mass. *Energy* **2016**, *111*, 991–1002. [CrossRef]
16. Halvgaard, R.; Poulsen, N.K.; Madse, H.; Jørgensen, J.B. Economic Model Predictive Control for Building Climate Control in a Smart Grid. In Proceedings of the 2012 IEEE PES Innovative Smart Grid Technologies (ISGT), Washington, DC, USA, 16–20 January 2012.
17. Pedersen, T.H.; Hedegaard, R.E.; Petersen, S. Space heating demand response potential of retrofitted residential apartment blocks. *Energy Build.* **2017**, *141*, 158–166. [CrossRef]
18. Masy, G.; Georges, E.; Verhelst, C.; Lemort, V.; Andre, P. Smart grid energy flexible buildings through the use of heat pumps and building thermal mass as energy storage in the Belgian context. *Sci. Technol. Built Environ.* **2015**, *21*, 800–811. [CrossRef]

19. Ingvarson, L.C.O.; Werner, S. Building mass used as short term heat storage. In Proceedings of the 11th International Symposium on District Heating and Cooling, Reykjavik, Iceland, 31 August–2 September 2008.

20. Kensby, J.; Trüschel, A.; Dalenbäck, J.-O. Potential of residential buildings as thermal energy storage in district heating systems—Results from a pilot test. *Appl. Energy* **2015**, *137*, 773–781. [CrossRef]

21. Patteeuw, D.; Bruninx, K.; Arteconi, A.; Delarue, E.; D'haeseleer, W.; Helsen, L. Integrated modeling of active demand response with electric heating systems coupled to thermal energy storage systems. *Appl. Energy* **2015**, *151*, 306–319. [CrossRef]

22. Papaefthymiou, G.; Hasche, B.; Nabe, C. Potential of Heat Pumps for Demand Side Management and Wind Power Integration in the German Electricity Market. *IEEE Trans. Sustain. Energy* **2012**, *3*, 636–642. [CrossRef]

23. Hedegaard, K.; Balyk, O. Energy system investment model incorporating heat pumps with thermal storage in buildings and buffer tanks. *Energy* **2013**, *63*, 356–365. [CrossRef]

24. Nyholm, E.; Goop, J.; Odenberger, M.; Johnsson, F. System benefits of demand response of space heating in Swedish single family dwellings. submitted for publication. 2017.

25. Pan, Z.; Guo, Q.; Sun, H. Feasible region method based integrated heat and electricity dispatch considering building thermal inertia. *Appl. Energy* **2017**, *192*, 395–407. [CrossRef]

26. Gu, W.; Wang, J.; Lu, S.; Luo, Z.; Wu, C. Optimal operation for integrated energy system considering thermal inertia of district heating network and buildings. *Appl. Energy* **2017**, *199*, 234–246. [CrossRef]

27. Li, P.; Wang, H.; Lv, Q.; Li, W. Combined Heat and Power Dispatch Considering Heat Storage of Both Buildings and Pipelines in District Heating System for Wind Power Integration. *Energies* **2017**, *10*, 893. [CrossRef]

28. Dominkovic, D.; Gianniou, P.; Münster, M.; Heller, A.; Rode, C. Utilizing thermal building mass for storage in district heating systems: Combined building level simulations and system level optimization. *Energy* **2018**, *153*, 949–966. [CrossRef]

29. Mata, E.; Kalagasidis, A.S.; Johnsson, F. A modelling strategy for energy, carbon, and cost assessments of building stocks. *Energy Build.* **2013**, *56*, 100–108. [CrossRef]

30. Nyholm, E. The role of Swedish single-family dwellings in the electricity system—The importance and impacts of solar photovoltaics, demand response, and energy storage. Ph.D. Thesis, Chalmers University of Technology, Gothenburg, Sweden, 2016.

31. Romanchenko, D.; Odenberger, M.; Göransson, L.; Johnsson, F. Impact of electricity price fluctuations on the operation of district heating systems: A case study of district heating in Göteborg, Sweden. *Appl. Energy* **2017**, *204*, 16–30. [CrossRef]

32. Langer, S.; Bekö, G. Indoor air quality in the Swedish housing stock and its dependence on building characteristics. *Build. Environ.* **2013**, *69*, 44–54. [CrossRef]

33. The National Board of Housing, Building and Planning. *Teknisk Status i den Svenska Bebyggelsen—Resultat Från Projektet BETSI*; Boverket: Karlskrona, Sweden, 2010.

34. Boverket—National Board of Housing, Building and Planning. "www.boverket.se" Boverket. Available online: https://www.boverket.se/en/start-in-english/ (accessed on 24 January 2018).

35. Statistics Sweden (SCB). Available online: http://www.scb.se/ (accessed on 6 November 2017).

36. Energimyndigheten. *Energistatistik för Lokaler 2010—Energy Statistics for Non-Residential Premises 2010*; Statens energimyndighet: Eskilstuna, Sweden, 2011.

37. Boverket. *Energi i Bebyggelsen—Tekniska Egenskaper Och Beräkningar—Resultat Från Projektet BETSI*; Boverket: Karlskrona, Sweden, 2010.

38. Bohm, B. On transient heat losses from buried district heating pipes. *Int. J. Energy Res.* **2000**, *24*, 1311–1334. [CrossRef]

39. Delmastro, C.; Martinsson, F.; Dulac, J.; Corgnati, S. Sustainable urban heat strategies: Perspectives from integrated district energy choices and energy conservation in buildings. Case studies in Torino and Stockholm. *Energy* **2017**, *138*, 1209–1220. [CrossRef]

40. Aronsson, S. *Fjärrvärmekunders Värme-Och Effektbehov—Analys Baserad På Mätresultat Från Femtio Byggnader*; Inst. för Energi & Miljö, Avd. Installationsteknik, Chalmers: Gothenburg, Sweden, 1996.

41. Göteborg Energi AB. "www.goteborgenergi.se". Available online: https://www.goteborgenergi.se/Files/dok/miljo/Milj%C3%B6v%C3%A4rden%20f%C3%B6r%20fj%C3%A4rrv%C3%A4rme%202015,%20Prelimin%C3%A4ra.pdf?TS=635895018252336533 (accessed on 23 November 2017).

42. Göteborg Energi AB. "https://grist.files.wordpress.com". 2009. Available online: https://grist.files.wordpress.com/2010/09/gothenburg,_sweden_i-district_energy_climate_award.pdf (accessed on 27 June 2017).

43. SMHI—Swedish Meteorological and Hydrological Institute. "http://strang.smhi.se/". Available online: http://strang.smhi.se/extraction/index.php (accessed on 24 November 2017).

44. Nord Pool. "http://www.nordpoolspot.com/". Available online: http://www.nordpoolspot.com/historical-market-data/ (accessed on 20 November 2015).

45. Energimyndigheten. *Energy in Sweden—Facts and Figures 2012*; Energimyndigheten: Eskilstuna, Sweden, 2012.

46. Nordenergi WG Taxes and Levies. *Nordic Tax Report 2013—Electricity Sector*; Nordenergi WG Taxes and Levies, 2014; Available online: https://www.energiauutiset.fi/media/energiauutiset/uutiset/2014/sk-14-nordenergi-tax-2013.pdf (accessed on 25 July 2019).

47. NVE/Energimyndigheten. *The Swedish-Norwegian Electricity Certificate Market—Annual Report 2012*; NVE/Energimyndigheten: Stockholm/Oslo, Sweden, 2013.

48. Grundsell, J. *Bottom-up Description of the Swedish Non-Residential Building Stock—Archetype Buildings and Energy Demand*; Chalmers ReproService: Göteborg, Sweden, 2013.

49. ISO 7730:2005. *Ergonomics of the Thermal Environment—Analytical Determination and Interpretation of Thermal Comfort Using Calculation of the PMV and PPD Indices and Local Thermal Comfort Criteria*; ISO: Geneva, Switzerland, 2005.

50. GÜNGÖR, G. *Thermal Comfort and Energy Consumption of A Typical Office Building*; Chalmers University of Technology: Gothenburg, Sweden, 2015.

51. Kensby, J. *Smart Energy Grids. Utilization of Space Heating Flexibility*; Chalmers University of Technology: Gothenburg, Sweden, 2017.

52. Lopes, R.A.; Chambel, A.; Neves, J.; Aelenei, D.; Martins, J. A literature review of methodologies used to assess the energy flexibility of buildings. *Energy Procedia* **2016**, *91*, 1053–1058. [CrossRef]

53. Mangold, M.; Österbring, M.; Wallbaum, H.; Thuvander, L.; Femenias, P. Socio-economic impact of renovation and energy retrofitting of the Gothenburg building stock. *Energy Build.* **2016**, *123*, 41–49. [CrossRef]

54. Hedbrant, J. *On the Thermal Inertia and Time Constant of Single-Family Houses*; Institute of Technology, Linköpings Universitet: Linköping, Sweden, 2001.

55. GAMS.com. GAMS Development Corporation. 2015. Available online: http://www.gams.com/dd/docs/solvers/cplex/#CPLEX_MIXED_INTEGER_PROGRAMMING (accessed on 26 June 2015).

56. Wouters, C.M. *Optimal Design and Regulation of Residential Distributed Energy Systems*; UCL (University College London): London, UK, 2016.

57. Edqvist, L. *Dispatch Modelling of A Regional Power Generation System*; Uppsala Universitet: Uppsala, Sweden, 2006; Available online: http://uu.diva-portal.org/smash/get/diva2:460501/FULLTEXT01.pdf (accessed on 25 July 2019).

58. Gadd, H.; Werner, S. Daily heat load variations in Swedish district heating systems. *Appl. Energy* **2013**, *106*, 47–55. [CrossRef]